

An optimal Mars Trojan asteroid search strategy

M. Todd^{1*}, P. Tanga², D. M. Coward³ and M. G. Zadnik¹

¹*Department of Imaging and Applied Physics, Bldg 301, Curtin University, Kent St, Bentley, WA 6102, Australia*

²*Laboratoire Cassiopée, Observatoire de la Côte d’Azur, BP 4229, 06304 Nice Cedex 04, France*

³*School of Physics, M013, The University of Western Australia, 35 Stirling Hwy, Crawley, WA 6009, Australia*

ABSTRACT

Trojan asteroids are minor planets that share the orbit of a planet about the Sun and librate around the L4 or L5 Lagrangian points of stability. Although only three Mars Trojans have been discovered, models suggest that at least ten times this number should exist with diameters ≥ 1 km. We derive a model that constrains optimal sky search areas and present a strategy for the most efficient use of telescope survey time that maximizes the probability of detecting Mars Trojans. We show that the *Gaia* space mission could detect any Mars Trojans larger than 1 km in diameter, provided the relative motion perpendicular to *Gaia*’s CCD array is less than 0.40 arcsec per second.

Key words: methods: numerical – methods: observational – minor planets, asteroids: general – planets and satellites: general – celestial mechanics

1 INTRODUCTION

Trojan asteroids are minor planets that share the orbit of a planet about the Sun and librate around the L4 and L5 Lagrangian points of stability. The L4 and L5 points are 60° ahead and behind, respectively, the planet in its orbit. Trojans represent the solution to Lagrange’s famous triangular problem and appear to be stable on long time-scales (100 Myr to 4.5 Gyr) (Pilat-Lohinger, Dvorak & Burger 1999; Scholl, Marzari & Tricarico 2005) in the N-body case of the Solar System. This raises the question whether the Trojans formed with the planets from the Solar nebula or were captured in the Lagrangian regions by gravitational effects. Studying the Trojans provides insight into the early evolution of the Solar System.

Since the discovery of the first Trojan in 1906 (Nicholson 1961) several thousand more have been found in the orbit of Jupiter. Among the terrestrial planets only Earth and Mars are known to have Trojans. While Earth has only a single known Trojan (2010 TK₇) which was discovered through examination of data from the WISE satellite (Connors, Wiegert & Veillet 2011), Mars presently has three known Trojans (5261 Eureka, 1998 VF₃₁ and 1999 UJ₇) listed by the Minor Planet Center. Previous modelling (Tabachnik & Evans 1999, 2000a,b) suggests that this number represents less than a tenth of the Mars Trojan (MT) population with diameter ≥ 1 km, and that there may be in excess of 100 with diameter ≥ 100 m.

Non-discovery of additional MTs may be attributed to a lack of observations targeting regions in which MTs could be

found, or their apparent motion being similar to inner Main Belt objects. Programmes to search for Near-Earth Asteroids (NEA) may flag objects with high apparent motion for further study while slower-moving objects are noted but may not be specifically followed up. NEA search regions are near the plane of the ecliptic and do not specifically target the entire region of stability for MTs. Observations are also limited to periods when the MT regions are visible from Earth. Other reasons for non-detection include the relatively small population, and orbital inclinations outside the plane of the ecliptic. Asteroids which could be Trojan candidates would not be flagged for further study by routine surveys because their apparent motions would not match the parameters of the survey for follow-up.

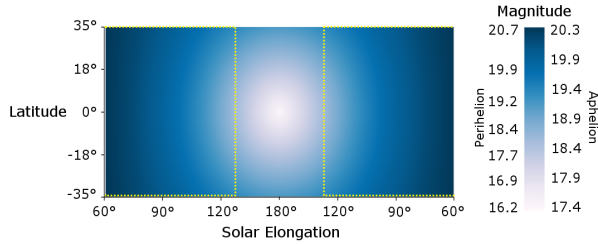
The spatial separation between the regions allows the L5 (trailing) region to be surveyed while Mars approaches opposition, and the L4 (leading) region surveyed when Mars has passed opposition. This affords a period of several months during which these regions could each be fully surveyed. Even with such relative flexibility in the available observing period, in contrast to searching for Earth Trojans (Todd et al. 2012b), it is still important to find the optimal strategy for efficient use of telescope time while maximizing sky coverage and probability of detection.

This paper employs a model probability distribution which we use to constrain optimal search areas and imaging cadences for efficient use of telescope time while maximizing the probability of detecting MTs. We examine in greater depth the case of detecting MTs from the initial study of inner planet Trojans (Todd, Coward & Zadnik 2012a).

* E-mail: michael.todd@icrar.org (MT)

Table 1. Absolute and apparent magnitudes at opposition, with apparent magnitudes for objects at perihelion and aphelion assuming eccentricity similar to that of Mars.

Class	Albedo	Diameter	Abs. mag. (<i>H</i>)	App. mag. (<i>V</i>)	
				Peri.	Aph.
S-class	0.203	1.0 km	17.35	16.2	17.4
		100 m	22.35	21.2	22.4
C-class	0.057	1.0 km	18.73	17.6	18.8
		100 m	23.73	22.5	23.8

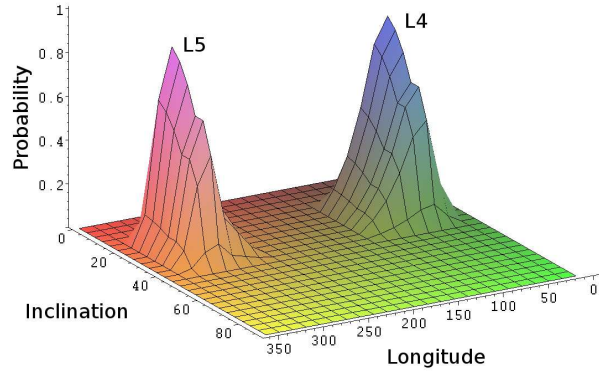
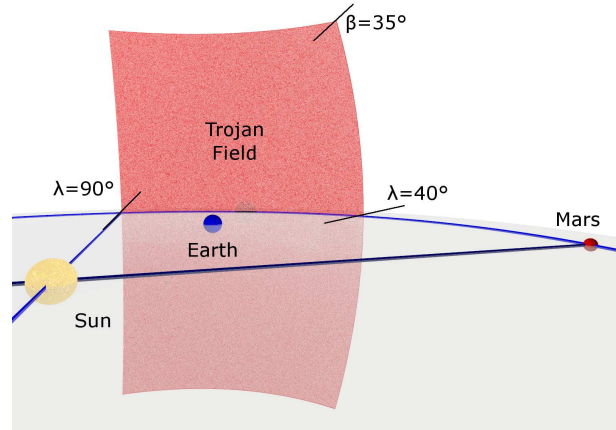
**Figure 1.** Apparent magnitude of a 1 km Mars Trojan by Solar Elongation and Heliocentric Latitude. Brightness ranges from $V = 17.4$ at opposition (180°) to $V = 20.3$ at a Solar elongation of 60° when the field is at aphelion, and ranges from $V = 16.2$ to $V = 20.7$ when the field is at perihelion. Elongations $\leq 135^\circ$ lie within *Gaia*'s scanning limit (yellow dotted line).

2 MODEL

Existing models (Tabachnik & Evans 1999, 2000a,b) provide estimates of MT populations, and some studies of the composition of known MTs have been made. Rivkin et al. (2003) found that (5261) Eureka and (101429) 1998 VF₃₁ are most likely Sa- or A-class asteroids, and that (121514) 1999 UJ₇ may be of X-class. This is an important consideration since albedo can vary greatly depending on composition. It is likely that other MTs will be relatively high albedo S-class (silicaceous) asteroids similar to NEAs and inner Main Belt asteroids, although there may be C-class (carbonaceous) asteroids. This affects the detection limit as S-class asteroids have a typical albedo of $p_v = 0.203$, X-class asteroids have $p_v = 0.174$ and C-class asteroids have $p_v = 0.057$ (Warner, Harris & Pravec 2009). In this paper calculations are made using these albedo values for S- and C-class asteroids to set limits on calculated magnitudes.

Calculations of absolute and apparent magnitudes at opposition using the methods described in Tedesco, Cellino & Zappala (2005) and Morais & Morbidelli (2002) are shown in Table 1, neglecting atmospheric extinction. Assuming S-class as the dominant class in the inner Solar System, and that an MT has an eccentricity similar to that of Mars, the apparent magnitude for an MT of 1 km diameter varies between $V = 16.2$ at opposition to $V = 20.7$ at a Solar elongation of 60° (Fig. 1) with the field at perihelion. An MT of 100 m diameter varies in magnitude between $V = 21.2$ to $V = 25.7$ across this elongation range in the same fashion. If the field is at aphelion the brightness ranges from $V = 17.4$ to $V = 20.3$ (1-km diameter), and $V = 22.4$ to $V = 25.3$ (100-m diameter).

Mikkola & Innanen (1994) found that MT orbits are

**Figure 2.** Probability distribution for Mars Trojan bodies by Inclination and Heliocentric Longitude (degrees). The figure shows peak detection probabilities for longitudes consistent with the classical Lagrangian points but that bodies, while co-orbital with Mars, are unlikely to be co-planar.**Figure 3.** Perspective illustration of Mars Trojan (L4) target field. The field ranges from Heliocentric longitude (λ) 40° to 90° and latitude (β) -35° to 35° . A complementary field exists in the trailing Lagrangian L5 region. This illustration represents the region in which Trojans are expected to be found, with the classical Lagrangian point at opposition.

only stable within the inclination ranges of $15^\circ \lesssim i \lesssim 30^\circ$ and $32^\circ \lesssim i \lesssim 44^\circ$ over an integration period of 4 Myr. Tabachnik & Evans (1999) mapped stable inclinations, finding that inclinations of $15^\circ \lesssim i \lesssim 30^\circ$ were more favourable. Scholl, Marzari & Tricarico (2005) refined this result, finding that objects with inclinations $\gtrsim 35^\circ$ become destabilized over longer periods. These orbit inclination models, and the heliocentric longitude model of Tabachnik & Evans (2000b), were used to identify regions where bodies are most likely to exist (Fig. 2).

The MT fields (Fig. 3) are bounded by the upper inclination limit of 35° and heliocentric longitude limits (FWHM) of $40^\circ \lesssim \lambda \lesssim 90^\circ$ (L4 region) and $270^\circ \lesssim \lambda \lesssim 320^\circ$ (L5 region). About ~ 69 per cent of projected bodies exist within these regions. We assume the distribution of bodies between the L4 and L5 regions is approximately equal.

The heliocentric solid angle of each MT field is 1.0 sr (3280 deg²). Calculation of the geocentric solid angle, neces-

sary for Earth-based observations, requires a transformation from the heliocentric reference. A numerical integration is performed using the solid angle integral described in Todd et al. (2012b) to determine the sky area for an Earth-based observer or a space-based instrument such as the *Gaia* satellite¹, which will be located near the Earth's L2 Lagrangian point (Mignard et al. 2007), for the observer's position relative to the field.

Calculations are made for Earth's longitude corresponding to the aphelion and perihelion longitudes of Mars' orbit to determine the upper and lower limits on maximum sky area. The calculated geocentric solid angles are 3.32 sr (10900 deg²) and 5.14 sr (16900 deg²) for the fields at opposition at aphelion and perihelion respectively. With the field centres at a Solar elongation of 60° the fields are 0.68 sr (2240 deg²) and 0.62 sr (2040 deg²) for Earth at Mars' aphelion and perihelion longitudes respectively. For *Gaia*, at the L2 Lagrangian point, these values differ by less than 1.5 per cent from the values calculated for Earth. Although *Gaia*'s orbit prevents observing regions at opposition, it will survey elongations from 45° to 135°.

3 TELESCOPE SURVEYS

The ability of current and proposed wide-field survey telescopes to survey the regions where Trojans are likely to be found in the orbits of Earth and Mars was first examined in Todd, Coward & Zadnik (2012a). It was found that the large sky area, particularly when the region is at opposition, would require a widefield telescope to survey the entire region. Attempting to complete such a survey in a single day was found to be time-consuming and inefficient.

Table 2 compares the relative capabilities of selected survey telescopes to cover the entire MT region at opposition and at a Solar elongation of 60°. We show that there exists up to eight-fold difference in area, and hence time required, between the region at opposition and at 60° elongation. Although the *Gaia* satellite has a narrow field-of-view (FOV), it has been included since it will operate in a continuous scanning mode and its orbit will enable it to image all of the sky to a Solar elongation of 45° (Mignard et al. 2007). *Gaia* will not be affected by the constraints of local horizon and airmass experienced by ground-based telescopes, however this advantage is mitigated by its limiting magnitude of $V = 20$.

The strategy of observing a swath of the region and progressively imaging the entire field over a period of time (Todd et al. 2012b) is suggested as an optimal method of searching for MTs. By imaging a swath of sky between the upper and lower latitude limits, the entire field can be surveyed over time as Earth (and Mars) revolves about the Sun. A single FOV-wide swath would be imaged in minutes by a survey telescope, as shown in Table 3. Whether the traditional approach of comparing images for moving object detection or flagging uncatalogued sources, the cadence is determined by the telescope FOV.

The relative geometry of Earth and Mars means that in a 2-year period Mars is not visible for about 3 months either

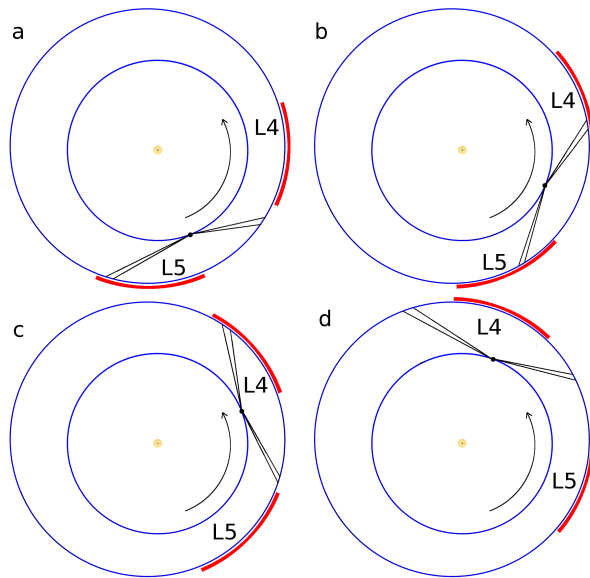


Figure 4. Observing a defined region of sky, with Earth's orbit about the Sun, implies the entire field can be imaged. The passage of time between each position from 4a to 4d is about 1.5 months.

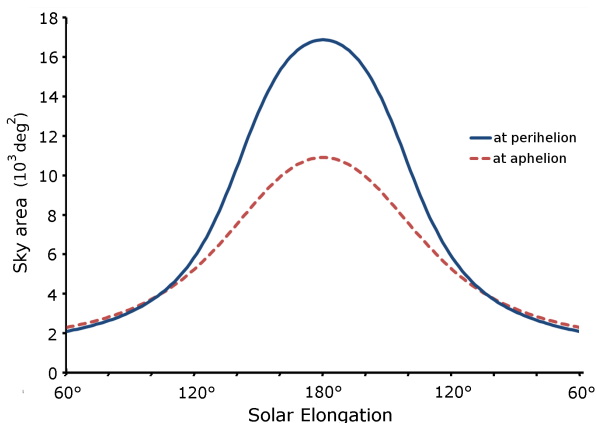


Figure 5. The sky area of each region varies from ~ 2000 deg² at a Solar elongation of 60° to 11000–17000 deg² at opposition (180°). The change in distance between Earth's and Mars' orbit, primarily due to Mars' eccentricity, significantly affects the sky area when the field is near opposition.

side of conjunction. The same applies to the MT fields, but also means the when the L4 field is at conjunction, then the L5 field is at least partly visible. This allows the fields to be surveyed over an extended period, or at different elongations in a synodic period. Defining specific regions and progressively observing the field over an extended period allows the entire field to be surveyed with efficient use of telescope time, and the observations accommodated around the primary science missions.

On approach to the trailing edge of the L5 MT region, observations can be made in the morning before sunrise. Thus end-of-night observations could be set to image across L5 on approach. When Mars is near opposition, morning observations can be made of the L4 region and evening observations can be set up to re-cover the L5 region. After the

¹ <http://gaia.esa.int>

Table 2. Comparison of different survey telescopes showing the required time to survey the entire field at opposition and at a Solar elongation of 60° . At opposition the sky area ranges from 10900 deg^2 (aphelion) to 16900 deg^2 (perihelion) while at an elongation of 60° it ranges from 2240 deg^2 (aphelion) to 2040 deg^2 (perihelion).

Telescope	Limiting mag.	Exposure	FOV	Opposition (FOVs)	Opposition (Time)	60° elongation (FOVs)	60° elongation (Time)	Instrument capabilities
Catalina	$V \sim 20$	30 s	8.0 deg^2	1360–2110	11.3h–17.6h	280–255	2.3h–2.1h	(Drake et al. 2009)
PTF 1.2 m	$R \sim 20.6$	60 s	8.1 deg^2	1345–2085	22.4h–34.8h	277–252	4.6h–4.2h	(Law et al. 2009)
Pan-STARRS	$R \sim 24$	30 s	7.0 deg^2	1555–2415	13.0h–20.1h	320–292	2.7h–2.4h	(Jedicke et al. 2007)
LSST	$r \sim 24.7$	30 s	9.6 deg^2	1135–1760	9.5h–14.7h	234–213	2.0h–1.8h	(Jones et al. 2009)
Gaia	$V \sim 20$	39.6 s^\dagger	0.69° -wide	160–195 ‡		55–50 ‡	330h–300h*	(Mignard et al. 2007)

† *Gaia* will operate in a continuous scanning mode where the CCD array will be read out at a rate corresponding to the angular rotation rate of the satellite (6h period).

‡ *Gaia*'s orbit parameters prevent observations within 45° of opposition. These values represent how many rotations it would take for *Gaia* to survey a region of this size. *Gaia*'s specific precession parameters are not considered so values should be considered as representative.

* Approximate time to complete sufficient rotations to scan across the entire field. The actual time spent scanning within the field will be a fraction of this value.

Table 3. Comparison of different survey telescopes showing the required time to survey a single swath of one CCD- or detector-width of the field at opposition compared to a Solar elongation of 60° . At opposition the height of the field ranges from 66° (aphelion) to 83° (perihelion) above the ecliptic plane while at an elongation of 60° the height is $\sim 30^\circ$.

Telescope	Opposition (FOVs)	Opposition (Time)	120° elongation (FOVs)	120° elongation (Time)	60° elongation (FOVs)	60° elongation (Time)
Catalina	47–59	23.5–29.5 min	37–46	18.5–23 min	21–22	10.5–11 min
PTF 1.2 m	47–59	47–59 min	37–46	37–46 min	21–22	21–22 min
Pan-STARRS	50–63	25–31.5 min	40–49	20–24.5 min	22–23	11–11.5 min
LSST	43–54	21.5–27 min	34–42	17–21 min	19–20	9.5–10 min
Gaia †		131–166 min ‡		104–130 min		60–61 min

† *Gaia* will operate in a continuous scanning mode where the CCD array will be read out at a rate corresponding to the angular rotation rate of the satellite (6h period). *Gaia*'s specific precession parameters are not considered so values should be considered as representative.

‡ *Gaia*'s orbit parameters prevent observations within 45° of opposition.

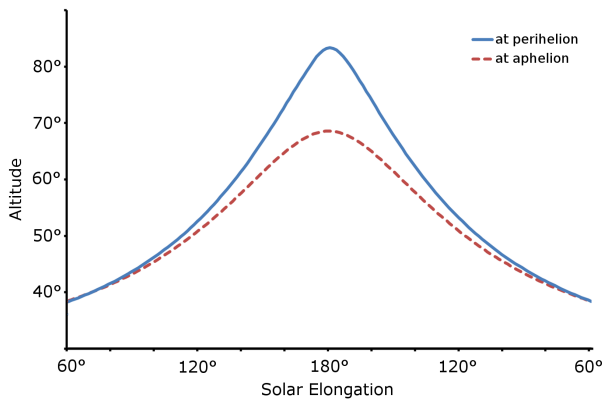


Figure 6. The angular height of the Mars Trojan field above (and below) the ecliptic plane from the geocentre at opposition ranges from 66° at aphelion, or 83° at perihelion, to $\sim 30^\circ$ at a Solar elongation of 60° .

L4 region has passed opposition evening observations can be made to re-cover that region. Morning observations will have ceased. The progression in Figure 4 shows how the MT regions might be surveyed as Earth passes by in its orbit.

Observations of MTs are time-limited only by the relative orbits of Earth and Mars. There will exist specific constraints particular to the geographic location of a telescope, depending on the relative positions of Earth and the

MT field. For example some Northern Hemisphere telescopes may not have access to the entire Southern part of the MT region described in Figure 3 when the field is near opposition, and the converse will apply to some Southern Hemisphere telescopes.

The limit adopted in this paper is that of Solar elongation of 60° , but with the MT regions each being visible for several months as Earth passes by, it is possible to survey the fields at a wide range of Solar elongations. If the observations are made at small elongations the available time is limited whereas at (or near) opposition the amount of sky area can be the limiting factor. Figure 5 shows the difference in sky area of the field between opposition and 60° elongation.

While a delay between follow-up images introduces other variations from such things as changes in atmospheric conditions and seeing, this could be compensated for by image convolution. Some telescopes are implementing image processing systems designed specifically for asteroid detection (e.g. Pan-STARRS+MOPS – Moving Object Processing System) (Jedicke et al. 2007). Depending on the relative positions of Earth and the MT field the apparent motion will vary with distance and direction.

Gaia's orbit dictates that it will scan narrow strips of the sky. As it will be a scanning instrument that performs a continuous scan by smooth and regular rotation of the spacecraft, follow-up observations for any object must be made by another instrument. Consequently a network of ground-

based telescopes, the *Gaia* Follow Up Network for Solar System Objects (Gaia-FUN-SSO)² is being established to provide follow-up observations after detection of Solar System objects.

The scanning law governing *Gaia*'s operation and the way the CCDs will operate (Tanga et al. 2008; Mignard 2010) limits the detection of Solar System objects as they cross the CCD array. With the 106.5° separation between lines of sight, motion in the 'across-scan' (AC) direction of 0.40 arcsec per second will cause an object to traverse one FOV-width and so have passed out of the FOV between the first and second observations of the field, even if starting at the edge of the CCD array on the first pass. An AC motion greater than 0.040 arcsec per second is larger than the pixel size in the AC direction and will cause smearing across pixels. Similarly, an 'along-scan' (AL) motion greater than 0.013 arcsec per second is larger than the pixel size in the AL direction. Since the motion of a Solar System object across the CCD depends on the relative positions of the object and *Gaia*, and the particular scanning orientation of *Gaia* at that time, these are important considerations for the design of the algorithms for detection of Solar System objects.

4 SUMMARY

Despite the thousands of known Jupiter Trojans, a mere handful of terrestrial Trojans have been discovered. There are only three known Mars Trojans, and the first Earth Trojan has only been very recently discovered (Connors, Wiegert & Veillet 2011). Simulations (Tabachnik & Evans 1999, 2000a,b) predict that this number constitutes about a tenth of the MT population with diameter ≥ 1 km. The prospect of detecting this population is limited by the size of the stable regions in which MTs can exist. However the Earth-Mars geometry offers an extended period over which a survey could be conducted. The conventional method of detecting asteroids by repeated observations of a field can be used, with a systematic approach to survey the entire MT field during a synodic period.

This study has identified the region of highest probability for detection, with an inclination $\leq 35^\circ$ and heliocentric longitude range of $40^\circ - 90^\circ$ (L4) and $270^\circ - 320^\circ$ (L5). Surveys of the entire field within the chosen limits are impractical on telescopes with small FOV but are possible on survey telescopes with sufficient FOV to accomplish the task in a single night, such as Catalina or the Large Synoptic Survey Telescope (LSST)³, when the field is at a Solar elongation $\lesssim 150^\circ$. In these cases it may be possible to survey the regions defined by the inclination limits. This would require the fields to be surveyed twice within a few days, as is common for Main Belt asteroids. Although possible, it is rather impractical as this occupies a significant amount of telescope time. When the field is at a Solar elongation $> 150^\circ$ the sky area becomes too large to be able to survey in a single night by any existing widefield telescope.

Given the challenges involved in attempting to survey

the entire field in a single session, we aimed to minimise the time requirement. Observing a swath of sky each session and progressively sampling the entire field over a synodic period achieves this aim. This approach requires minimal time each session by making a single pass across the field. By repeating this at intervals which provides an overlap of the telescope FOV from one pass to the next the common regions of consecutive images can be compared.

The sky areas for Earth-based observers at different Solar elongations have been determined using the numerical integrations described in Todd et al. (2012b). A strategy has been proposed for observing a sub-region of the MT field and, as Earth revolves about the Sun, redefining this region and progressively surveying the entire field during a synodic period. This approach takes only a few minutes per night at intervals of 3–4 days. This approach requires the observed region to be redefined at intervals to progressively observe the entire field over those months when the field is visible from Earth.

Since the field is visible during the majority of one synodic period (about two years), nights lost due to adverse weather conditions can be rescheduled without critically impacting the timing of the programme. The flexibility in the timing allows such a programme to be more readily accommodated alongside the primary science mission, and is readily achievable by a survey telescope. While this method requires a program of continued observations over several months, the total time commitment for the program is a few tens of hours spread over that period.

The *Gaia* satellite, at Earth's L2 Lagrangian point, will survey the MT fields as part of its larger mission to survey the whole sky. With a detection limit of $V = 20$, *Gaia* can be expected to detect MTs larger than 1 km diameter, provided the lateral motion across the CCD array is less than 0.40 arcsec per second. As with any uncatalogued Solar System object detected by *Gaia*, these would need to be followed up by ground-based telescopes.

The specific observing geometry of the *Gaia* satellite at Earth's L2 Lagrangian point will be examined in more detail in future work. Initial simulations for *Gaia*'s detection of inner Solar System Trojans in the orbits of Earth and Mars show promise. Results of detailed simulations will be reported with particular regard to the detection limits and observational mode of operation of *Gaia*.

ACKNOWLEDGMENTS

MT thanks the organizers of the *Gaia* Solar System Science workshop (held in Pisa, Italy, 2011) for providing a fertile environment for discussing *Gaia* science. DMC is supported by an Australian Research Council Future Fellowship.

REFERENCES

- Connors M., Wiegert P., Veillet C., 2011, *Nat*, 475, 481
- Drake A. J. et al., 2009, *ApJ*, 696, 870
- Jedicke R., Magnier E. A., Kaiser N., Chambers K.C., 2007, in Milani A., Valsecchi G. B., Vokrouhlick D., eds, *Proc. IAU Symp. 236, Near Earth Objects, our Celestial Neighbours: Opportunity and Risk*. Kluwer, Dordrecht, p. 341

² <http://www.imcce.fr/gaia-fun-sso/>

³ The LSST is still in the development phase (www.lsst.org).

- Jones R. L. et al., 2009, *Earth Moon Planet*, 105, 101
 Law N. M. et al., 2009, *PASP*, 121, 1395
 Mignard F. et al., 2007, *Earth Moon Planet*, 101, 97
 Mignard F., 2010, *Adv. Space Res.*, 47, 356
 Mikkola S., Innanen K., 1994, *AJ*, 107, 1879
 Morais M. H. M., Morbidelli A., 2002, *Icarus*, 160, 1
 Nicholson S. B., 1961, *Astron. Soc. Pac. Leaflets*, 8, 239
 Pilat-Lohinger E., Dvorak R., Burge Ch., 1999, *Celest. Mech. Dyn. Astron.*, 73, 117
 Rivkin A. S. et al., 2003, *Icarus*, 165, 349
 Scholl H., Marzari F., Tricarico P., 2005, *Icarus*, 175, 397
 Tabachnik S., Evans N. W., 1999, *ApJ*, 517, L63
 Tabachnik S., Evans N. W., 2000a, *MNRAS*, 319, 63
 Tabachnik S., Evans N. W., 2000b, *MNRAS*, 319, 80
 Tanga P., Hestroffer D., Delbo M., Frouard J., Mouret S., Thuillot W., 2008, *Planet. Space Sci.*, 56, 1812
 Tedesco E. F., Cellino A., Zappala V., 2005, *AJ*, 129, 2869
 Todd M., Coward D. M., Zadnik M. G., 2012a, *Planet. Space Sci.*, doi: 10.1016/j.pss.2011.11.002
 Todd M., Tanga P., Coward D. M., Zadnik M. G., 2012b, *MNRAS*, 420, L28
 Warner B. D., Harris A. W., Pravec P., 2009, *Icarus*, 202, 134